



An experimental study of novel nanofluids based on deep eutectic solvents (DESs) by Choline chloride and ethylene glycol



Kimia Jafari^a, Mohammad Hossein Fatemi^{a,*}, Luis Lugo^{b,*}

^aChemometrics Laboratory, Department of Chemistry, University of Mazandaran, Babolsar, Iran

^bCINBIO, Universidade de Vigo, Grupo GAME, Departamento de Física Aplicada, 36310 Vigo, Spain

ARTICLE INFO

Article history:

Received 8 February 2022

Revised 9 May 2022

Accepted 30 May 2022

Available online 1 June 2022

Keywords:

Nanofluid

Deep eutectic solvent

MgO

Thermophysical properties

Choline chloride

ABSTRACT

In this work, the preparation and characterization of some new nanofluids based on deep eutectic solvents (DESs) consisting of a hydrogen bond acceptor, ethylene glycol (EG), and a hydrogen bond donor, choline chloride (ChCl), as well as water, are presented. The nanofluids were designed by the dispersion of spherical MgO nanoparticles in four different DESs, ChCl:EG (molar ratio of 1:2), 1ChCl:5EG, 1ChCl:2EG:2Water, and 1ChCl:5EG:2Water. The stability of nanofluids was carried out by measuring size distribution for five days, which discovered the best results obtained with nanofluids of dispersed MgO in DES 1ChCl:5EG. Thermophysical properties (thermal conductivity and density) were measured and the influence of nanoparticles' mass fraction, temperature, and water content all were examined. The acquired outcomes revealed that the trend of density was reducing by increment in temperature since for pure base fluids and DES-based nanofluids 1.3% decrement were recorded, averagely (the decline in density was sharper in the case of DES 1ChCl:5EG and its based nanofluids). The thermal conductivity was almost constant during the range of 283.15–333.15 K. It confirmed that the thermal conductivities of prepared nanofluids based on DESs with water were higher in comparison to the ones based on DESs without water and nanoparticles concentration could promote thermal conductivity. The greatest enhancement was gained at 10 wt% of MgO suspended in DES 1ChCl:2EG. The isobaric thermal expansivity was also determined at different temperatures. Eventually, the general conclusions were drawn and concerning the results, the MgO/DES 1ChCl:2EG 10 wt% nanofluids was introduced as the most efficient.

© 2022 The Authors. Published by Elsevier B.V.

1. Introduction

Nowadays, it's crystal clear that the nanofluids are more useful for heat transfer applications rather than the conventional liquids. This matter encourages scholars to develop and improve different aspects of these compounds. One of the most efficient factors on defining the thermophysical characteristics of such fluids is the nature of the base fluid. In an attempt to overcome the limited liquid range and/or poor thermal stability of some conventional used solvents (e.g. mineral oil and alcohol), ionic liquids (ILs) have introduced as a candidate because of their favorable properties such as diversity, high boiling point, and low pressure [1–6]. Concomitantly, these solvents indicate some innate worriment in particular high-cost, tedious process of preparation, and toxicity in some ones [5].

With an intention of finding more preferable options, deep eutectic solvents (DESs) as a new generation of ILs, which have been widely investigated. These homogeneous solvents, which are prepared with an ordinary procedure through the formation of hydrogen bond between two basic ingredients (a donor and an acceptor of hydrogen bond), are known with prominent aspects such as low-priced, soluble, non-volatile, low melting point, bio-compatible, and non-toxic [7–9], which are worthy to appraise as attractive substitutes. In addition, some of the most leading reported applications of DESs are as follows: significant in the synthesis of carbon nanotubes [10,11], well-known eco-friendly solvents used for extraction [12,13], applicable for catalysis [14], dopamine sensor [15], and electro-polishing [16,17], and also utilization as a medium for metal oxides dissolution [18]. Besides these aforementioned applications, the present potential, and perspective of expected applications DESs have been discussed by Marcus [19] and Tome et al. [20]. Employing of DESs as a heat transfer fluid is subjected to study in recent times. Aimed at addressing the impact of graphene surface modification on stability and properties of nanofluids, Liu et al. [21] were fabricated

* Corresponding authors.

E-mail addresses: mhfatemi@umz.ac.ir (M. Hossein Fatemi), luis.lugo@uvigo.es (L. Lugo).

Nomenclature

ChCl	Choline Chloride	IL	Ionic liquid
CNT	Carbon nanotube	MgO	Magnesium oxide
DES	Deep eutectic solvent	MTPB	Methyl triphenylphosphonium bromide
DLS	Dynamic light scattering	SDG	Silica decorated graphene
EG	Ethylene glycol	TC	Thermal conductivity
FT-IR	Fourier-transform infrared spectroscopy	TEG	Triethylene glycol
HBA	Hydrogen bond acceptor		
HBD	Hydrogen bond donor		

some DES-based nanofluids by dispersion of silica decorated graphene (SDG) in ethylene glycol (EG)-choline chloride (ChCl) systems. It was demonstrated that the trend of nanofluids viscosity was increased with expanding nanoparticles' concentration in the range from 298 K to 308 K, while at 308–323 K temperature range was reduced owing to the interaction between DES and nanoparticles. Moreover, the maximum thermal conductivity (TC) enhancement (11.26%) was reported for 3 wt% SDG nanofluids based on 1ChCl:2EG.

Fang et al. [22] introduced stable nanofluids constructed of functionalized graphene oxide (0.01, 0.02, and 0.05 wt%) suspended in phosphonium and ammonium-based DESs through an ultrasonic technique. The authors found that the synthesized nanofluids showed no explicit sedimentation for four weeks as respects nanofluids' stability was followed via visual observation, optical microscopy, and zeta potential analysis. By experimental investigation, they revealed that nanofluids based on methyltriphenylphosphonium bromide (MTPB) and EG (1:5 M ratio) showed a 177% improvement in TC.

In an interesting study, Walvekar et al. [23] were used MTPB, ChCl, EG, and triethylene glycol (TEG) as ingredients in order to form eleven different DESs. Then, by the suspension of CNT in 0.04 wt% concentration, DES-based nanofluids were fabricated without any stabilizer. They employed differential scanning calorimetry to analyze freezing points and other properties such as weight loss, vapor pressure, and thermal degradation were evaluated via a thermo-gravimetric analyzer. Additionally, by virtue of Friedman and Avrami's models, the degradation reaction order was defined. The authors reported that activation energy, thermal stability, and kinetic parameters were improved in nanofluids than base solvents. More details and case studies of DESs utilization to prepare nanofluids were reviewed comprehensively in the paper of Jafari et al. [9].

The present paper is devoted to provide an experimental analysis on preparation of MgO nanofluids based on DESs composed of ChCl, a cheap and biodegradable raw component as hydrogen bond acceptor (HBA), and EG, a generic polyol with somewhat low viscosity as HBD. Then, the impact of distinct parameters (i.e. concentration of nanoparticle, temperature, and addition of water in DES construction) on thermophysical properties such as density and thermal conductivity of pure DESs (with and without water) and considered nanofluids are analyzed experimentally and discussed in detail.

2. Materials and methods

2.1. Materials

All chemicals to perform this defined project were provided in high grade, so the procedure of preparation of DESs and DES-based nanofluids was carried out without any further purifica-

tion. The essential information of the materials used in the current project is summarized in Table 1, as reported by their suppliers.

2.2. Preparation of DESs.

In order to the preparation of binary DESs, the required amount of ChCl and EG was weighted by a Sartorius electronic balance (CPA225, Sartorius AG, Göttingen, Germany) with an uncertainty of 1×10^{-5} g with regard to the considered molar ratios (1:2 and 1:5). The proper mixtures of ChCl and EG were heated and stirred at 80 °C with 800 rpm until a transparent solvent was achieved. In the second step, ternary mixtures based on the addition of water were prepared to consider the effect of water content on DESs properties. These aqueous DESs were prepared in molar ratios of 1ChCl:2EG:2Water and 1ChCl:5EG:2Water. All formed DESs and their aqueous mixtures form homogenous solvents.

2.3. Nanofluids preparation

On the subject of nanofluids preparation through a two-step method with different nanoparticle mass fractions (1, 5, and 10 wt%), related required amounts of MgO were first weighed and then dispersed in proper weight of each DESs separately. Next, to the purpose of achieving a well-disperse nanofluid and to break down the possible agglomerates of nanoparticles within the base fluids, the samples were placed under an ultrasound probe at 35 kHz for a time period of 40 min. The basic information of all studied DESs and related nanofluids is indicated in Table 2. The preparation procedure of DESs and DES-based nanofluids is summarized graphically in Fig. 1.

3. Results and discussion

3.1. FT-IR analysis of DESs

In order to explore the structure and functional groups of prepared DESs, the prepared DESs and their components (EG and ChCl) were subjected to FT-IR analysis using a Nicolet 6700 spectrometer (detector of DTGS KBr and beam splitter of KBr) with high resolution at room temperature. All spectra were recorded over the wavenumber range of 4000 to 400 cm^{-1} . The obtained FT-IR spectra of DESs were represented in Fig. 2, also the detailed spectra of each component (ChCl and EG) were provided in figure S1 (Supplementary materials). The observed broadband at 3308 cm^{-1} is a representation of the O-H functional group, which confirmed the formation of hydrogen bonds between ChCl and EG. This band is stronger in the case of 1:5 M ratios of ChCl and EG (DES B) and is located at 3315 cm^{-1} . The band of N-H stretching bonding was recorded for ChCl (see Fig. S1 in supplementary materials) at 3010 cm^{-1} . It can be observed from Fig. 2, that a blue shift has happened by changing the location from 3010 cm^{-1} to 3026 and 3029 cm^{-1} , for DES A and DES B, respectively. Regarding that

Table 1
Specifications of the chemicals used for the preparation of DESs and nanofluids (NFs).

Name	Formula	Molar mass/g.mol ⁻¹	Purity	Lot #	Source
Ethylene glycol	C ₂ H ₆ O ₂	62.07	≥ 99.5%	H1730	Honeywell
Choline Chloride	C ₅ H ₁₄ ClNO	139.62	≥ 98%	WXBD2533V	SIGMA-ALDRICH
Magnesium Oxide	MgO	40.304	≥ 99%	GR1305	PlasmaChem GmbH

Table 2
The prepared DESs and DES-based nanofluids with their abbreviations.

Sample	Component	Molar ratio	ϕ_m	Abbreviation
Binary DESs	ChCl + EG	1:2	–	DES A
	ChCl + EG	1:5	–	DES B
Ternary DESs	ChCl + EG + Water	1:2:2	–	DES AW
	ChCl + EG + Water	1:5:2	–	DES BW
Nanofluids	MgO in DES A	1:2	1 wt%	MgO/A 1 wt%
			5 wt%	MgO/A 5 wt%
			10 wt%	MgO/A 10 wt%
	MgO in DES B	1:5	1 wt%	MgO/B 1 wt%
			5 wt%	MgO/B 5 wt%
			10 wt%	MgO/B 10 wt%
	MgO in DES AW	1:2:2	5 wt%	MgO/AW 5 wt%
	MgO in DES BW	1:5:2	5 wt%	MgO/BW 5 wt%

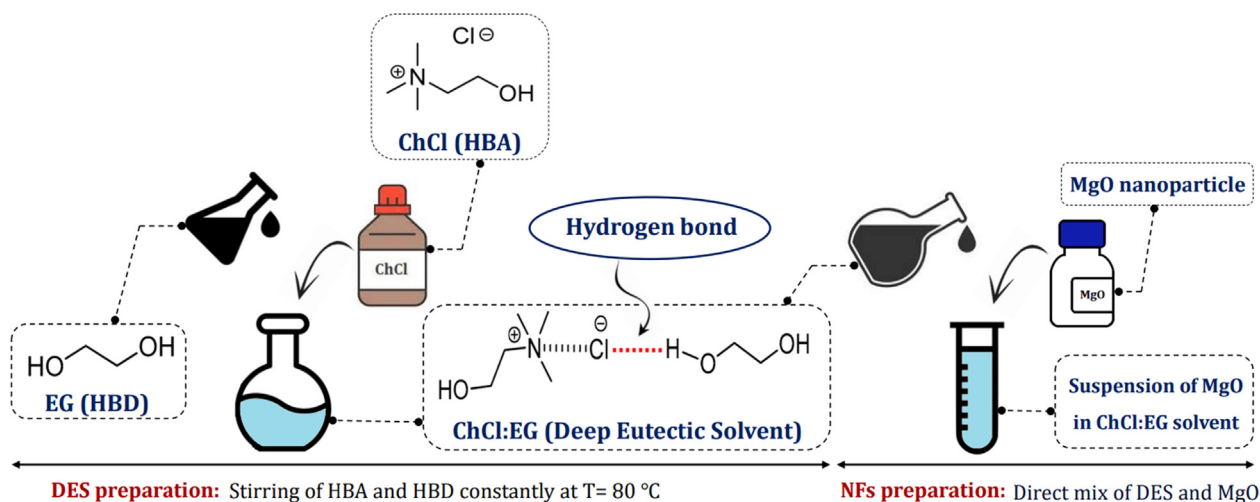


Fig. 1. Graphical illustration of the preparation procedure of DES and DES-based nanofluids.

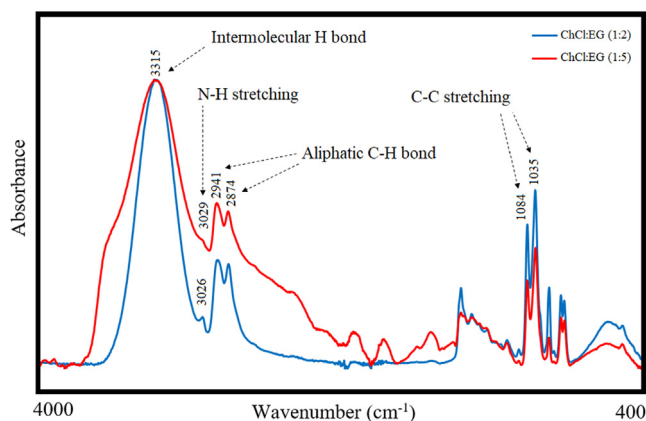


Fig. 2. FT-IR spectrum of prepared DES A (1ChCl:2EG) and DES B (1ChCl:5EG).

higher wavenumber means higher energy, it seems that the increase in N-H stretching energy was because of a reduction of intermolecular hydrogen bonds in ChCl, which made possible the

formation of hydrogen bonds in the ChCl:EG system. The bands between 2850 and 3000 cm⁻¹ are deputed of stretching modes of aliphatic C-H bonds (CH₂ and CH₃), while the bending modes emerged at 1415–1480 cm⁻¹ and 1322–1370 cm⁻¹. Moreover, the medium pointed bands at 1135 and 1084 cm⁻¹ are represented the C-C bond stretching vibration.

3.2. Stability

As a means to assign the stability of nanofluids, dynamic light scattering (DLS) was employed to define the distribution size of nanoparticles within the different base fluids using a Zetasizer Nano ZS (Malvern, United Kingdom) with a scattering angle of 173°. In order to perform DLS tests, several samples of MgO nanoparticles dispersed in different DESs were prepared. Ideally, a stable nanofluid is appointed by a unimodal size distribution curve with a narrow peak. Herein, the samples were analyzed over five days in both static (still condition) and dynamic (using ultrasonic bath and shaker) situations. Fig. 3 illustrates the obtained results of DLS analysis on the first and fifth days.

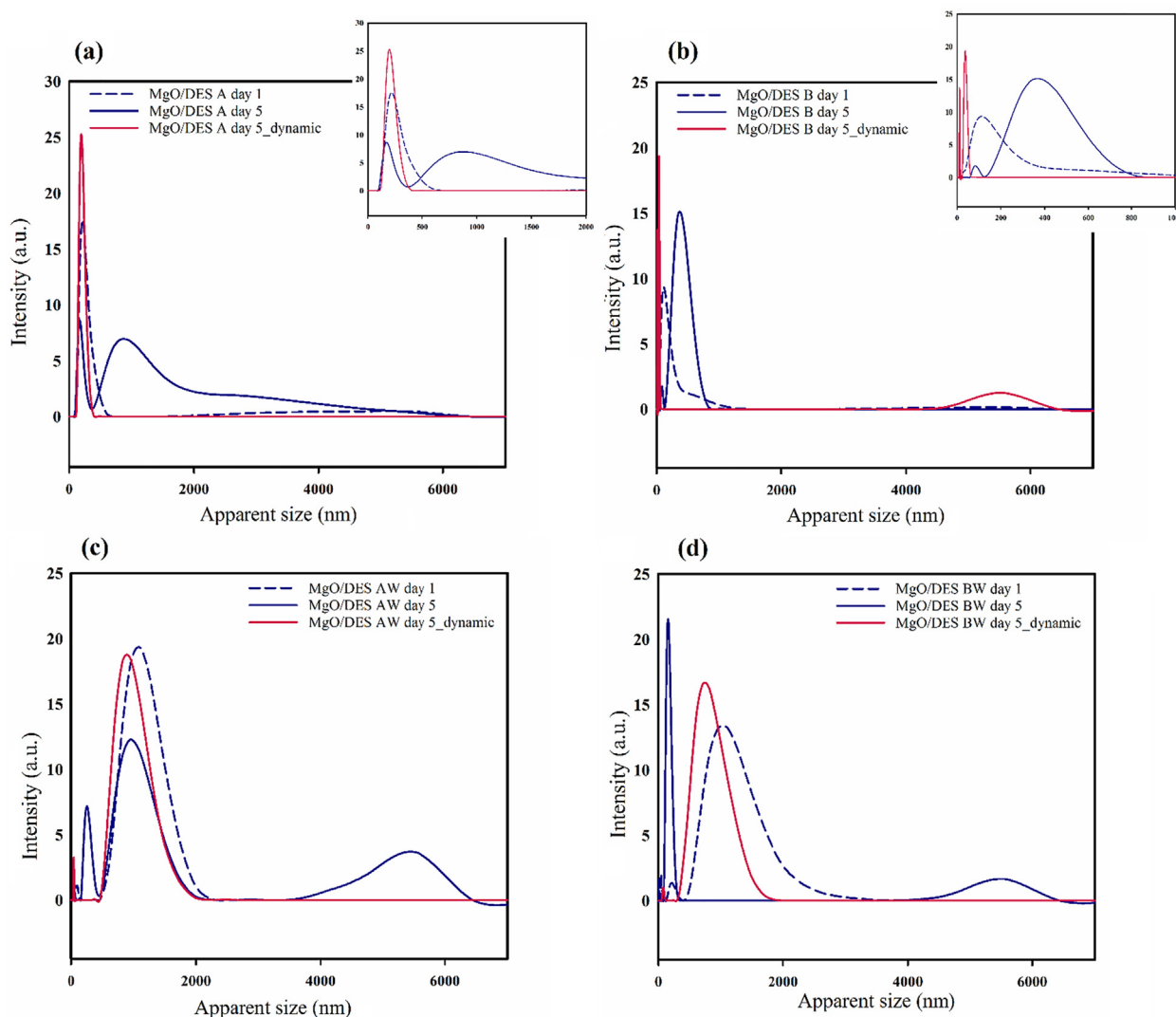


Fig. 3. The obtained results of DLS analysis for (a) MgO/DES A, (b) MgO/DES B, (c) MgO/DES AW, and (d) MgO/DES BW nanofluids.

It is predictable that the stability of suspensions will decrement over time, especially on the assumption of still ones as far as there wasn't any extra addition to stabilizing nanofluids. As can be revealed from Fig. 3, the changes in size distribution in static samples were confirmed by multi-modal and wide peaks in the case of MgO/DES A (a) and MgO/DES AW (c), while the variations in size distribution in dynamic conditions were much better, which was evident by decreasing of average apparent size in particular for MgO/DES B (b). With regard to Fig. 3, it can be observed that the obtained size distribution showed uni-modal and narrow curves in dynamic samples; among all, it can mention the suspension of MgO nanoparticles in DES B (Fig. 3-C) was more dispersed than others.

3.3. Thermophysical properties of DESs and DES-based nanofluids

3.3.1. Density

All density measurements were carried out by Anton Paar DMA 501 (Graz, Austria) vibrating-tube densimeter for all samples; the tested temperature range was 288.15–313.15 K and measured every five degrees, also the setup was rinsed by milli-Q water and ethanol and then dried completely, before each test. Further, the density of DES-based nanofluids were subjected to test. It can be seen from Fig. 4, that the density of DESs and DES-based

nanofluids, displays a decreasing trend versus the temperature increment. Generally, the density of a compound reduces at higher temperatures, which arises from thermal expansion. It's expected this fact would be the reason for the observed behaviour. It can be observed that the addition of water in DESs combination caused a decrement in the values of density. Considering the coverage factor of 2, the declared expanded uncertainty of density measurement is considered lower than 0.1%.

One of the crucial required properties for the usage of nanofluids in engineering applications is thermal expansivity. The isobaric thermal expansivity is determined by the derivatives of polynomial density adjustments according to the following equation [24–26]:

$$\alpha_p = - \left(\frac{1}{\rho} \right) \left(\frac{\partial \rho}{\partial T} \right)_p$$

which α_p , T , P , ρ and are isobaric thermal expansivity, temperature, pressure, and density, respectively.

The determined values of isobaric thermal expansivities of pure DESs and different loaded nanofluids are gathered in Table 3 at four temperatures. With regard to the survey of obtained data, it can be found isobaric thermal expansivities increases as temperature rises. These enhancements were approximately observed in the range of 3% to 8% for the base fluids and nanofluids, respectively

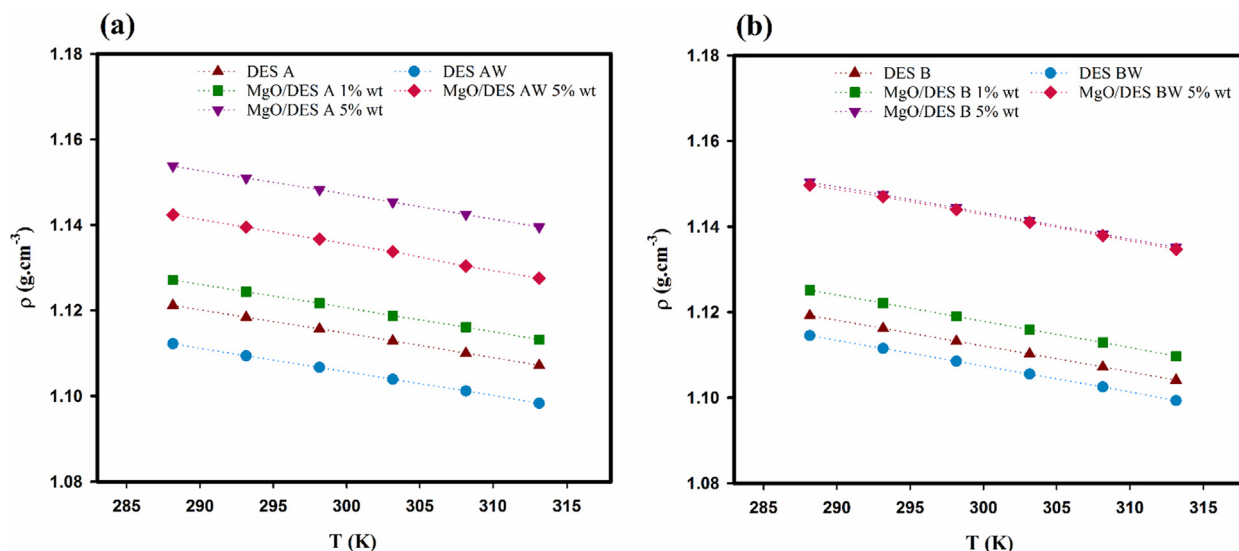


Fig. 4. The trend of density versus temperature for (a) DES A (with and without water) and their related nanofluids, (b) DES B (with and without water) and their related nanofluids.

Table 3
Experimental values of density and the determined isobaric Thermal Expansivity for studied samples.

T/K	DES A		DES AW		DES B			DES BW		
	$\phi_m = 0$	$\phi_m = 0.01$	$\phi_m = 0.05$	$\phi_m = 0$	$\phi_m = 0.05$	$\phi_m = 0$	$\phi_m = 0.01$	$\phi_m = 0.05$	$\phi_m = 0$	$\phi_m = 0.05$
288.15	1.1212	1.1272	1.1538	1.1122	1.1424	1.1192	1.1252	1.1504	1.1145	1.1497
293.15	1.1184	1.1244	1.1510	1.1094	1.1395	1.1162	1.1221	1.1475	1.1115	1.1470
298.15	1.1157	1.1217	1.1483	1.1067	1.1367	1.1132	1.1190	1.1444	1.1085	1.1440
303.15	1.1129	1.1188	1.1454	1.1039	1.1338	1.1102	1.1159	1.1414	1.1055	1.1410
308.15	1.1100	1.1161	1.1425	1.1012	1.1304	1.1072	1.1129	1.1383	1.1025	1.1379
313.15	1.1072	1.1132	1.1396	1.0983	1.1276	1.1041	1.1097	1.1352	1.0993	1.1347
	$10^4 \cdot \alpha_p / K^{-1}$									
293.15	4.93	4.92	4.81	4.94	5.05	5.35	5.50	5.21	5.35	4.97
298.15	4.99	4.97	4.91	4.99	5.18	5.40	5.52	5.29	5.43	5.17
303.15	5.06	5.01	5.00	5.03	5.31	5.45	5.54	5.37	5.51	5.36
308.15	5.12	5.05	5.09	5.08	5.45	5.49	5.56	5.44	5.59	5.56

Expanded uncertainty of density ($k = 2$): 0.1%.

Expanded uncertainty of isobaric thermal expansivity ($k = 2$): 4%.

Expanded uncertainty of temperature ($k = 2$): 0.1 K.

in the case of DES A, and 3% to 12% in the case of DES B. Increments in the values of α_p versus temperature for ternary-based nanofluids were higher than binary-ones for both DES AW and BW. A major degree of cohesion is reached in relation to pure DESs but the relation of $-\left(\frac{\partial \rho}{\partial T}\right)_p$ remains positive [27]. In addition, it can be concluded the α_p reduces by increasing nanoparticle loading for nanofluids.

3.3.2. Thermal conductivity

The thermal conductivity (TC) of base fluids and nanofluids was subjected to test using a THW-L2 TC-meter (Thermtest Inc., Canada) at 283.15, 298.15, and 333.15 K. The total reported data of TC are the mean value of three replicates. The expanded uncertainty ($k = 2$) of TC measurements is 5% [28]. There are many potentially effectual parameters on nanofluids TC such as temperature, nanoparticle's type, shape, concentration and size, pH, nature of base fluid and any extra additives [29,30]. Figs. 5 and 6 represent graphically the TC data and the enhancements, achieved in each case. Most experimental findings [6,31] of nanofluids with even low volume fractions of nanoparticles represented that TC of nanofluid will augment when compared to the base solvent. As it can be observed from Fig. 5, with the suspension of MgO nanoparticles into the DES A and DES B, a remarkable increment in TC is

obtained, and as expected this TC enhancement has a direct relation with the mass fraction of MgO. The value of nanofluids' TC moved up from 0.223 to 0.273, and 0.242 to 0.288 W/m.K⁻¹ from 1 wt% to 10 wt% at 298.15 K for MgO/DES A, MgO/DES B, respectively. This trend is consistent with the reported observations in the relevant literature [21,32–34]. Some outlines may account for this fact such as: hydrodynamics effects associated with Brownian motion have only a minor effect on the TC of the nanofluid, thermal diffusion is much faster than nanoparticle Brownian motion. Brownian motion has an active role in generating a cluster of particles, which could improve TC in a way with a particular meaning, but other effects such as interfacial resistance, nature and aspect ratio of agglomerates dictate such enhancement in nanofluids [35].

Taking into account the inevitable character of water (because of high polarity, water is capable to act as an acceptor and donor of hydrogen bonding, thus, it is anticipated to expose strong intermolecular interactions with DES constituents [7]), ternary DESs (AW and BW) and ternary-based nanofluids were considered and their TC values were analysed in order to the assessment of the water content effect. Averagely, by the addition of water in DES chemical construction, TC was enhanced around ~8% by DES AW while this improvement was around ~4% in the case of DES BW.

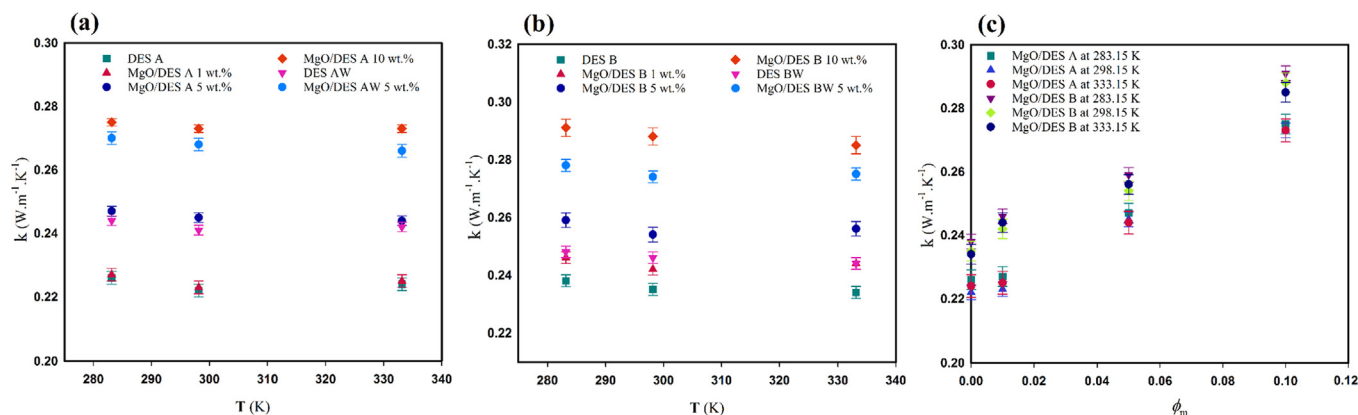


Fig. 5. The graphical representation of TC-temperature (a) DES A, DES AW, and their related nanofluids, (b) DES B, DES BW, and their related nanofluids, and (c) TC-mass fraction of nanoparticles.

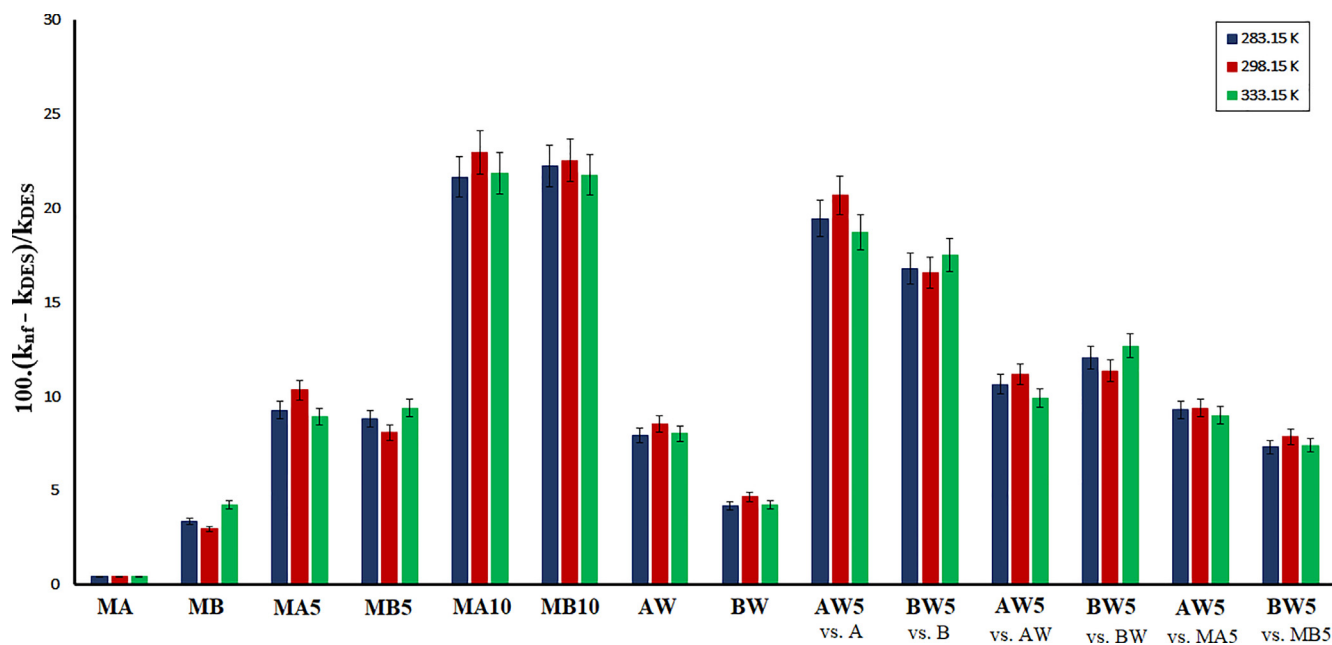


Fig. 6. The enhancement of thermal conductivity in different comparison. (MA: MgO/DES A 1 wt%, MB: MgO/DES B 1 wt%, MA5: MgO/DES A 5 wt%, MB5: MgO/DES B 5 wt%, MA10: MgO/DES A 10 wt%, MB10: MgO/DES B 10 wt%, AW: pure DES AW, BW: pure DES BW, AW5: MgO/DES AW 5 wt%, BW5: MgO/DES BW 5 wt%).

Thus, the outcomes were confirmed that TC is increased in the cases of DES AW and BW compare to the DES A and B. It can be mentioned that addition of water through two possible mechanisms causes an augmentation in thermal conductivity; first, the unique chemical structure of H₂O makes highly provide the hydrogen bond formation (which is vital for DES creation) and reduces viscosity of final formed aqueous solvent than relevant binary one. The motion of nanoparticles, here MgO, is more facile in a less viscous base fluid, thereby transfer of heat and mass is increased. The second scenario arises from the intrinsic and remarkable characteristic of water in thermal conductivity, which leads to shift TC towards higher values. Further, the variation of TC values were observed from 0.241 to 0.269, and 0.246 to 0.274 W/m.K⁻¹ from pure base fluids (DES AW and DES BW) to 5 wt% MgO/AW, and MgO/BW, respectively. It should be stated that it's not truly easy to judge in fairness the impact of competition of water addition and nanoparticles loading on TC improvements. Considering DESs are composed of at least two components, HBA and HBD, changing each ingredient not only would change the thermophysical properties of solvents but also may cause a mutation in pH values, which

is effective on the stability of suspensions by influencing charges of nanoparticle surface and thereby affecting TC enhancement. Towards a precise pursuit of DESs chemical structure impact on TC, some tractable experiments employing the same nanoparticles subject to different DESs (variable in each component) are required and suggested to supply further detailed information.

The observed independency of thermal conductivities to temperature is in accordance with the reported behavior of DES-based nanofluids in the literature [21,32–34]. As it can be observed, the TC improvements at 283.15 K were considerable. These improvements are comparable with the results reported by Siong et al. [36] (nanofluids of dodecyl-benzene sulfonic acid doped polyaniline nanoparticles in DES ChCl:Urea), and Liu et al. [21] (dispersions of SDG in 2EG:1ChCl base solvent), which reported 11.06% as maximum TC enhancement. Also, Dehury et al. [33] reported average TC increases up to 8% for 1 wt% loaded alumina nanoparticles in DES consisting of MTPB and EG in a temperature range of 293–333 K.

The possible enhancement percentage of all considered nanofluids compare to the pure binary DESs, pure ternary DESs,

and binary-based nanofluids are represented in Fig. 6. The highest TC enhancement obtained $\sim 23\%$ for MgO/DES A 10 wt% and the lowest enhancement was $\sim 0.6\%$ for MgO/DES A 1 wt%. It is worth mentioning that MgO-nanofluids based on ternary DESs represented an interesting improvement in comparison to those based on binary DESs since MgO/DES AW 5 wt% showed $\sim 9\%$ rather than MgO/DES A 5 wt%, and MgO/DES BW 5 wt% exhibited $\sim 7\%$ compared to MgO/DES B 5 wt%. In addition, TC increment for these mentioned ternary-based nanofluids observed around 19.5% and 17% contrasted to DES A and DES B, respectively.

4. Conclusion

With the aim of developing green alternative materials, novel nanofluids based on DESs were designed and experimentally investigated. The most prominent results of the present contribution are summarized as follows: First, two binary DESs and two ternary DESs composed of choline chloride (ChCl), ethylene glycol (EG) and water were prepared in molar ratios of 1:2, 1:5, 1:2:2 and 1:5:2. Then, various new nanofluids were introduced by dispersion of MgO nanoparticles in DESs with mass fractions of 1, 5, and 10 wt %. Second, density and thermal conductivity (TC) of nanofluids were explored experimentally, while it was confirmed by stability analysis that samples show well-dispersion. At the end, nanofluid of 10 wt% MgO in 1ChCl:5EG demonstrated the highest TC enhancement (23%), whilst no clear TC improvement was reached by 1 wt% MgO in 1ChCl:2EG.

Taking into account an explicit increment in TC was observed caused by the water presence in DESs chemical structure, a controllable investigation using extra aqueous DESs is highly recommended to provide more detailed results of effect competition of water addition and nanoparticles loading on TC enhancement.

Declaration of Competing Interest

The authors declare that they have no known competing financial interests or personal relationships that could have appeared to influence the work reported in this paper.

Acknowledgments

K.J. is appreciated GAME group of Universidade de Vigo to provide materials and experimental facilities. L.L. acknowledges of grant PID2020-112846RB-C21 funded by MCIN/AEI/10.13039/501100011033, grant PDC2021-121225-C21 funded by MCIN/AEI/10.13039/501100011033 and by "European Union NextGenerationEU/PRTR", project ENE2017-86425-C2-1-R by "Ministerio de Economía y Competitividad" (Spain) and FEDER program. Funding for open access charge: Universidade de Vigo/CISUG.

Appendix A. Supplementary material

Supplementary data to this article can be found online at <https://doi.org/10.1016/j.molliq.2022.119521>.

References

- [1] M. Sheikholeslami, S.A. Shehzad, Z. Li, Water based nanofluid free convection heat transfer in a three dimensional porous cavity with hot sphere obstacle in existence of Lorenz forces, *Int. J. Heat Mass Transf.* 125 (2018) 375–386, <https://doi.org/10.1016/j.ijheatmasstransfer.2018.04.076>.
- [2] Y. Guo, T. Zhang, D. Zhang, Q. Wang, Experimental investigation of thermal and electrical conductivity of silicon oxide nanofluids in ethylene glycol/water mixture, *Int. J. Heat Mass Transf.* 117 (2018) 280–286, <https://doi.org/10.1016/j.ijheatmasstransfer.2017.09.091>.
- [3] J.-H. Qin, Z.-Q. Liu, N. Li, Y.-B. Chen, D.-Y. Wang, A facile way to prepare CuS-0il nanofluids with enhanced thermal conductivity and appropriate viscosity, *J. Nanoparticle Res.* 19 (2) (2017), <https://doi.org/10.1007/s11051-017-3743-8>.

- [4] P. Bose, D. Deb, S. Bhattacharya, Ionic liquid based nanofluid electrolytes with higher lithium salt concentration for high-efficiency, safer, lithium metal batteries, *J. Power Sources.* 406 (2018) 176–184, <https://doi.org/10.1016/j.jpowsour.2018.10.050>.
- [5] A.A. Minea, S.M.S. Murshed, A review on development of ionic liquid based nanofluids and their heat transfer behavior, *Renew. Sustain. Energy Rev.* 91 (2018) 584–599, <https://doi.org/10.1016/j.rser.2018.04.021>.
- [6] S. Hamze, D. Cabaleiro, P. Estellé, Graphene-based nanofluids: A comprehensive review about rheological behavior and dynamic viscosity, *J. Mol. Liq.* 325 (2021) 115207, <https://doi.org/10.1016/j.molliq.2020.115207>.
- [7] T. El Achkar, S. Fourmentin, H. Greige-Gerges, Deep eutectic solvents: An overview on their interactions with water and biochemical compounds, *J. Mol. Liq.* 288 (2019) 111028, <https://doi.org/10.1016/j.molliq.2019.11.1028>.
- [8] N.F. Gajardo-Parra, M.J. Lubben, J.M. Winnert, A. Leiva, J.F. Brennecke, R.I. Canales, Physicochemical properties of choline chloride-based deep eutectic solvents and excess properties of their pseudo-binary mixtures with 1-butanol, *J. Chem. Thermodyn.* 133 (2019) 272–284, <https://doi.org/10.1016/j.jct.2019.02.010>.
- [9] K. Jafari, M.H. Fatemi, P. Estellé, Deep eutectic solvents (DESs): A short overview of the thermophysical properties and current use as base fluid for heat transfer nanofluids, *J. Mol. Liq.* 321 (2021) 114752, <https://doi.org/10.1016/j.molliq.2020.114752>.
- [10] M.K. AlOmar, M.A. Alsaadi, T.M. Jassam, S. Akib, M. Ali Hashim, Novel deep eutectic solvent-functionalized carbon nanotubes adsorbent for mercury removal from water, *J. Colloid Interface Sci.* 497 (2017) 413–421, <https://doi.org/10.1016/j.jcis.2017.03.014>.
- [11] J. Zhong, L. Li, M. Waqas, X. Wang, Y. Fan, J. Qi, B.o. Yang, C. Rong, W. Chen, S. Sun, Deep eutectic solvent-assisted synthesis of highly efficient PtCu alloy nanoclusters on carbon nanotubes for methanol oxidation reaction, *Electrochim. Acta.* 322 (2019) 134677, <https://doi.org/10.1016/j.electacta.2019.134677>.
- [12] N. Pavlović, S. Jokić, M. Jakovljević, M. Blažić, M. Molnar, Green extraction methods for active compounds from food waste - Cocoa bean shell, *Foods.* 9 (2020) 1–15, <https://doi.org/10.3390/foods9020140>.
- [13] E. Shabani, D. Zappi, L. Berisha, D. Dini, M.L. Antonelli, C. Sadun, Deep eutectic solvents (DES) as green extraction media for antioxidants electrochemical quantification in extra-virgin olive oils, *Talanta* 215 (2020) 120880, <https://doi.org/10.1016/j.talanta.2020.120880>.
- [14] A.E. Ünlü, A. Arlkaya, S. Takaç, Use of deep eutectic solvents as catalyst: A mini-review, *Green Process. Synth.* 8 (2019) 355–372, <https://doi.org/10.1515/gps-2019-0003>.
- [15] C.M.A. Brett, Deep eutectic solvents and applications in electrochemical sensing, *Curr. Opin. Electrochem.* 10 (2018) 143–148, <https://doi.org/10.1016/j.coelec.2018.05.016>.
- [16] A.A. Kityk, V.S. Protsenko, F.I. Danilov, O.V. Kun, S.A. Korniy, Electropolishing of aluminium in a deep eutectic solvent, *Surf. Coatings Technol.* 375 (2019) 143–149, <https://doi.org/10.1016/j.surfcoat.2019.07.018>.
- [17] W.O. Karim, A.P. Abbott, S. Cihangir, K.S. Ryder, Electropolishing of nickel and cobalt in deep eutectic solvents, *Trans. Inst. Met. Finish.* 96 (4) (2018) 200–205, <https://doi.org/10.1080/00202967.2018.1470400>.
- [18] J. Richter, M. Ruck, Synthesis and dissolution of metal oxides in ionic liquids and deep eutectic solvents, *Molecules* 25 (2020) 1–32, <https://doi.org/10.3390/molecules25010078>.
- [19] Y. Marcus (Ed.), *Deep Eutectic Solvents*, Springer International Publishing, Cham, 2019.
- [20] L.I.N. Tomé, V. Baião, W. da Silva, C.M.A. Brett, Deep eutectic solvents for the production and application of new materials, *Appl. Mater. Today.* 10 (2018) 30–50, <https://doi.org/10.1016/j.apmt.2017.11.005>.
- [21] C. Liu, P. Jiang, Y. Huo, T. Zhang, Z. Rao, Experimental study on ethylene glycol/choline chloride deep eutectic solvent system based nanofluids, *Heat Mass Transf.* (2021), <https://doi.org/10.1007/s00231-021-03030-z>.
- [22] Y.K. Fang, M. Osama, W. Rashmi, K. Shahbaz, M. Khalid, F.S. Mjalli, M.M. Farid, Synthesis and thermo-physical properties of deep eutectic solvent-based graphene nanofluids, *Nanotechnology.* 27 (7) (2016) 075702, <https://doi.org/10.1088/0957-4484/27/7/075702>.
- [23] R. Walvekar, Y.Y. Chen, R. Saputra, M. Khalid, H. Panchal, D. Chandran, N.M. Muabarak, K.K. Sadasivuni, Deep eutectic solvents-based CNT nanofluid – A potential alternative to conventional heat transfer fluids, *J. Taiwan Inst. Chem. Eng.* 128 (2021) 314–326, <https://doi.org/10.1016/j.jtice.2021.06.017>.
- [24] K. Brzóška, B. Józwiak, A. Golba, M. Dzida, S. Boncel, Thermophysical properties of nanofluids composed of ethylene glycol and long multi-walled carbon nanotubes, *Fluids.* 5 (4) (2020) 241, <https://doi.org/10.3390/fluids5040241>.
- [25] E. Sani, J.P. Vallejjo, D. Cabaleiro, L. Lugo, Functionalized graphene nanoplatelet-nanofluids for solar thermal collectors, *Sol. Energy Mater. Sol. Cells.* 185 (2018) 205–209, <https://doi.org/10.1016/j.solmat.2018.05.038>.
- [26] D. Cabaleiro, M.J. Pastoriza-Gallego, C. Gracia-Fernández, M.M. Piñero, L. Lugo, Rheological and volumetric properties of TiO₂-ethylene glycol nanofluids, *Nanoscale Res. Lett.* 8 (2013) 1–13, <https://doi.org/10.1186/1556-276X-8-286>.
- [27] J.P. Vallejjo, J. Pérez-Tavernier, D. Cabaleiro, J. Fernández-Seara, L. Lugo, Potential heat transfer enhancement of functionalized graphene nanoplatelet dispersions in a propylene glycol-water mixture. Thermophysical profile, *J. Chem. Thermodyn.* 123 (2018) 174–184, <https://doi.org/10.1016/j.jct.2018.04.007>.
- [28] J.I. Prado, U. Calviño, L. Lugo, Experimental Methodology to Determine Thermal Conductivity of Nanofluids by Using a Commercial Transient Hot-

- Wire Device, Appl. Sci. 12 (1) (2022) 329, <https://doi.org/10.3390/app12010329>.
- [29] L. Yang, W. Ji, J.-N. Huang, G. Xu, Xu, An updated review on the influential parameters on thermal conductivity of nano-fluids, J. Mol. Liq. 296 (2019) 111780, <https://doi.org/10.1016/j.molliq.2019.111780>.
- [30] T. Ambreen, M.-H. Kim, Influence of particle size on the effective thermal conductivity of nanofluids: A critical review, Appl. Energy. 264 (2020) 114684, <https://doi.org/10.1016/j.apenergy.2020.114684>.
- [31] J.P. Vallejo, J.I. Prado, L. Lugo, Hybrid or mono nanofluids for convective heat transfer applications. A critical review of experimental research, Appl. Therm. Eng. 203 (2022) 117926, <https://doi.org/10.1016/j.applthermaleng.2021.117926>.
- [32] Y.Y. Chen, R. Walvekar, M. Khalid, K. Shahbaz, T.C.S.M. Gupta, Stability and thermophysical studies on deep eutectic solvent based carbon nanotube nanofluid, Mater. Res. Express. 4 (7) (2017) 075028, <https://doi.org/10.1088/2053-1591/aa77c7>.
- [33] P. Dehury, A.K. Upadhyay, T. Banerjee, Evaluation and conceptual design of triphenylphosphonium bromide-based deep eutectic solvent as novel thermal nanofluid for concentrated solar power, Bull. Mater. Sci. 42 (6) (2019), <https://doi.org/10.1007/s12034-019-1946-6>.
- [34] C. Liu, H. Fang, X. Liu, B. Xu, Z. Rao, Novel Silica Filled Deep Eutectic Solvent Based Nanofluids for Energy Transportation, ACS Sustain. Chem. Eng. 7 (24) (2019) 20159–20169, <https://doi.org/10.1021/acssuschemeng.9b0617910.1021/acssuschemeng.9b06179.s001>.
- [35] P.D. Shima, J. Philip, B. Raj, Role of microconvection induced by Brownian motion of nanoparticles in the enhanced thermal conductivity of stable nanofluids, Appl. Phys. Lett. 94 (2009) 2007–2010, <https://doi.org/10.1063/1.3147855>.
- [36] C.T. Siong, R. Daik, M.A.A. Hamid, Thermally conductive of nano fluid from surfactant doped polyaniline nanoparticle and deep eutectic ionic liquid, AIP Conf. Proc. 1614 (2014) 381–385, <https://doi.org/10.1063/1.4895227>.